



Contents lists available at ScienceDirect

Engineering Failure Analysis

journal homepage: www.elsevier.com/locate/engfailanal

Development of a fatigue life prediction methodology for welded steel semi-trailer components based on a new criterion



L. Tello^a, L. Castejon^{a,*}, H. Malon^a, D. Valladares^a, P. Luque^b, Daniel A. Mantaras^b,
D. Ranz^a, J. Cuartero^a

^a Department of Mechanical Engineering, University of Zaragoza, c/Maria de Luna s/n 50.018, Zaragoza, Spain

^b Department of Construction and Manufacturing Engineering, University of Oviedo, c/Pedro Puig Adam 7-1^a 33.203, Gijón, Spain

ARTICLE INFO

Keywords:

Fatigue life
Weibull distribution
Welded joints
Semitrailer
Axle support

ABSTRACT

This paper presents a procedure developed to predict the fatigue life in components made of steel, based on the mechanical properties of the base material and Thermally Affected Zones (TAZs) owing to welding. The fatigue life cycles of the studied components are obtained based on a certain survival probability provided by a Weibull distribution. This procedure is thought to be applied on semi-trailer components, and therefore it is proposed for the steels that are typically used in its manufacturing. A criterion for the adjustment of the exponent and the stress stroke of the fatigue life curve in welded joints is proposed in which the parameters that define the alternating stress versus the number of cycles to failure (S-N) curve are obtained exclusively from the ratio between the base material yield stress of a given steel and the strength of its Thermally Affected Zone. This procedure is especially useful for steels that do not have a complete characterization of their fatigue parameters. These developments are implemented in a subroutine that can be applied in commercial codes based on Finite Element Method (FEM) to obtain a fatigue life prediction. Finally, a numerical-experimental validation of the developed procedure is carried out by means of a semi-trailer axle bracing support fatigue analysis.

1. Introduction

At present, there is a tendency toward the development of lightened semi-trailer vehicles [1] thanks to improvements in the design and the application of new materials such as high-strength steels and aluminum alloys. A series of advantages are derived from such improvements, including the reduction of polluting emissions, fuel savings, better dynamic behavior, greater vehicle stability, a lower tendency to overturn, an increase in payload, better performance, and the reduction of maintenance costs.

To produce optimized semi-trailer vehicles, structural steels with higher strength properties than traditional ones are being applied to a greater extent, with a reasonable cost and ease for the manufacturing process and component welding. Knowledge of the behavior of the materials used in the manufacture of semi-trailer vehicles not only in static conditions but also under dynamic loads and fatigue is essential for the design process and prediction of the vehicle's long-term durability [2].

To accurately predict the fatigue life of semi-trailer components, first, an experimental characterization of the monotonic properties of some reference steels was conducted. Second, the maximum strength of the thermally affected zones (TAZs) produced by the welding process in those steels was determined by Vickers hardness tests [3]. Third, the fatigue behavior of the reference steels was predicted as a function of the monotonic properties, based on Wöhler curves [4] and the Basquin's equation [5]. There are

* Corresponding author.

E-mail address: luiscast@unizar.es (L. Castejon).

<https://doi.org/10.1016/j.engfailanal.2019.104268>

Received 28 January 2019; Received in revised form 17 September 2019; Accepted 4 November 2019

Available online 26 November 2019

1350-6307/ © 2019 The Authors. Published by Elsevier Ltd. This is an open access article under the CC BY-NC-ND license (<http://creativecommons.org/licenses/by-nc-nd/4.0/>).

different methods for obtaining the fatigue behavior of the base steel based on this equation, such as the Mischke method [6], SAE method [14], linear logarithmic adjustment method explained by Besa and Giner [15], method of Shigley [16], and Jvinal method [17]. However, considering that the load cycles in a semi-trailer fluctuate, the correction method developed by Morrow [18] was applied, to consider the effect of the mean stress on the fatigue life prediction. There are numerous criteria for fatigue life prediction in metallic materials. A few of these prediction criteria are based on different modifications of the Basquin–Manson [19] and –Coffin [20] equations. The universal slope method [21] and the four-point correlation [22] were chosen as the criteria to obtain the fatigue parameters of the steels studied. Fourth, for the fatigue life prediction criteria for welded joints, Malon stated in his doctoral thesis [16] that the International Institute of Welding (IIW) [17,18] offers the best results for fatigue life in the TAZs produced by the welding process, and this will be the criterion applied in this study.

Other authors, such as Schjødt–Thomsen and Andreassen [19], analyzed the low cycle fatigue behavior of welded T-joints in high strength steel, and they stated that the Manson–Coffin methodology with data predicted from static material data were proven to provide accurate results compared with the experimental fatigue results presented.

Given the highly statistical nature of the fatigue analysis in this study, an investigation was conducted to determine whether the Weibull distribution [20,21] is an adequate tool for estimating survival based on the reliability of fatigue life predictions. To this end, the Herd–Johnson method [22] was applied to determine the percentage of failures that occur before the time corresponding to the fatigue life range. It was considered necessary to perform fatigue life tests on overlapped welded specimens with the three different configurations of material analyzed, to determine whether the results obtained fit well with a Weibull distribution. The statistical R-software [23] was to be employed to obtain the parameters of the Weibull distribution of each of the specimen configurations in each load case. The estimators were obtained, for both the scale parameter and the form or profile parameter of the Weibull distribution, and the adjustment accuracy tests were conducted on the experimental data with the Weibull distributions obtained using the maximum likelihood method [24] and the Anderson–Darling test [25], instead of other possible tests such as those proposed by Karl Pearson [26] and Kolmogorov–Smirnov [27].

The present article shows a methodology for the design and prediction of the semi-trailer fatigue life and specifically of its components, which are manufactured by welding different steels. Numerical analysis techniques are applied to reduce experimental testing as much as possible [28].

However, the key point of this study is that a new criterion is developed to predict fatigue life, based on the International Institute of Welding criteria and by applying the necessary corrections, depending on the properties of each material base and its properties after the welding process, particularly in the TAZs in the welded joint. The procedure presented in this study was developed to be implemented in the process of calculation and optimization against fatigue of the welded joints existing in steel-built semi-trailers. Manufacturing companies should therefore have complete knowledge of the monotonic properties of the applied steels, maximum strength of the TAZs generated by the welding process between those steels, a prediction of the fatigue behavior of the steels including the corresponding fatigue parameters, and the complete definition of the fatigue life prediction criterion for welded joints. After developing this huge work by the manufacturing companies, the fatigue life testing curve of the welded specimens for each combination of welded steels will be determined. Evidently, the amount of work involved to obtain each curve for two determined welded steels between components of a welded semi-trailer is very high. Therefore, to substantially reduce this amount of work, this article presents an adjustment model that allows the modification of fatigue life prediction curves based on the work of the IIW, focusing on two steel parameters. In particular, the base material yield stress and the strength of the TAZ. Both parameters are easily determined and allow the definition of the fatigue life transformed curve for a null mean load. Therefore, significant time and effort could be saved with the proposed model, called Tello–Castejon adjustment model. This procedure is intended to be particularly useful for steels that do not have a complete characterization of their fatigue parameters.

The developed criterion for fatigue life prediction is validated by laboratory testing on welded specimens, and also by testing of a complex subassembly such as the subset of an axle bracing support of a semi-trailer.

In order to apply the fatigue life prediction procedure for welded steel semi-trailer components in a user-friendly manner based on the new prediction criteria developed, a post-process subroutine was implemented. This post-process subroutine is able to predict the fatigue life with a pre-established prediction reliability for each of the applied load cases. This subroutine is executed from a friendly user interface integrated with the calculation code.

Finally, a fatigue test is carried out with a semi-trailer axle bracing, including two support types. The test is developed on a bench, and it is verified that the predictions made by the developed methodology establish the fatigue life number of reversals that adjust to the experimentally measured values.

2. Experimental characterization of monotonic properties of steels S235JR, S355MC and S500 MC

First, an experimental characterization of the monotonic properties of the materials S235JR, S355MC, and S500MC was carried out, given that they are frequently applied steels in semi-trailer construction. These steels comply with the provisions of the PNE-prEN 10149-2 [29] and PNE-prEN 10027-2 regulations [30].

The Young's modulus of the S235JR, S355MC, and S500MC steels was first obtained by means of tensile tests carried out by an INSTRON 8032 test machine, as shown in Fig. 1. Testing specimens are shown in Fig. 2 after the experimental procedure. Six repetitions were performed for each batch of test samples to obtain the mean value and the determination coefficient (R^2), which is a measure of how well a given variable can be predicted using a linear function of a set of other variables.

A static-type extensometer with a gauge length of 25 mm and maximum allowed displacement of 12.5 mm was used to measure the Young's modulus of the materials studied, which can be seen in Fig. 3 (see Table 1).



Fig. 1. Universal testing machine used for tensile tests.



Fig. 2. Typology of specimens used for tensile tests.



Fig. 3. Extensometer used to obtain Young's modulus.

Table 1
Young's modulus and R^2 values for tested steels.

Steel	Young's modulus (MPa)	R^2
S235JR	216,975	0,939
S355MC	217,193	0,963
S500MC	218,295	0,957

R_m values obtained in this way match the values provided by the steel manufacturers and the corresponding standard. In particular, for S235JR steel R_m is between 360 and 510 MPa, for S355MC steel 510–680 MPa, and for S500MC steel 540–720 MPa [Table 2](#).

Table 2
Engineering and Ultimate Tensile Strength for tested steels.

Steel	R _e Engineering Strength (MPa)	R _m Ultimate Strength (MPa)
S235JR	290.73	55,566
S355MC	359.70	624.52
S500MC	492.10	647.00

3. Vickers hardness tests for equivalent maximum strength determination of Thermally Affected Zones by welding process

The heat input that takes place in the areas near the weld bead or TAZ causes changes in the microstructure of steel, and consequently there are changes in the monotonic properties of the material [19,31]. A change in the fatigue strength occurs as a result of this variation in the monotonic properties. It is essential to mechanically characterize the TAZ, given that manufacturers of semi-trailer vehicles know that the possible fatigue cracks in a vehicle appear in these areas.

Fig. 4 shows a scheme that corresponds to a typical distribution of Thermally Affected Zones in a butt-welded specimen. In this figure, four clearly differentiated Thermally Affected Zones (TAZ1, TAZ2, TAZ3, and TAZ4), and the Base Material Zone (BMZ) can be observed.

The number of Thermally Affected Zones that are considered will vary depending on the required degree of continuity to be obtained on the results based on the Finite Element Method.

To characterize the mechanical properties in the TAZs, a Matsuzawa MXT 50 microdurometer was used, as shown in Fig. 5.

The regulations followed to perform the hardness tests were UNE-EN ISO 6507-1: 2018 [3] and UNE-EN ISO 9015-1: 2011 [32]. The temperatures at the time of testing varied between 21 °C and 23 °C, which is a permitted range within the established limits by the regulation (between 10 °C and 35 °C).

The butt-welded specimens that were analyzed were made in different material combinations (S235JR-S235JR, DX355MC-DX355MC, and S235JR-DX355MC), as shown in Fig. 6. The results obtained of the Vickers Hardness measurements are shown in Figs. 7–9.

In addition, hardness tests were performed on four T-shaped welded specimens whose material configuration is shown in Fig. 10. These T-shaped welded specimens had a weld bead on each side of the web. The web was made of S355MC steel with dimensions of 100 × 50 mm and a thickness of 4.5 mm. The flange was made of S235JR steel with dimensions of 250 × 50 mm and a thickness of 10 mm. This kind of sample configuration aims to emulate some of the common weld joints in three-axle semitrailers such as those in the junction zone between the bracing supports and the longitudinal beams, or even the joints of the King-Pin bridge.

A Vickers hardness test was carried out once the necessary preparations were made. Two lines of 15 indentations each were made in each test sample such that the hardness was measured in the base materials in the Thermally Affected Zone and in the weld bead. Macrographs of the specimens, as well as the indentation lines for the four tested specimens, can be seen in Fig. 11.

The Vickers hardness measured along the two indentation lines in the four specimens is shown in Figs. 12 and 13.

In the present study, a single Thermally Affected Zone was considered. The values were grouped into five different groups corresponding to the base material S235JR (points 1–3), Thermally Affected Zone of steel S235JR (points 4–6), base material of steel S355MC (points 13–15), Thermally Affected Zone of S355MC (points 10–12), and finally to the weld bead (points 7–9). Therefore, the mean values and their equivalence in strength, listed in Table 3, were obtained according to the UNE-EN ISO 18,265 [33] standard.

Once the hardness values of Thermally Affected Zones were obtained by means of Vickers hardness tests, an equivalent elastic limit of each Thermally Affected Zone was calculated in order to obtain the stress-strain curve for each material based on the following assumptions:

- The slopes of the elastic and plastic zones remain the same, respectively, as the slopes of the elastic and plastic area of the base material.
- It was considered that the area under the stress-strain curve would be the same for the base material and for the corresponding Thermally Affected Zone. That is to say, the deformation energy density for each material was kept constant.

The bilinear curves of the Thermally Affected Zones of each material were calculated by taking into account these hypotheses. The bilinear curves for the TAZs of S235JR, S355MC, and S500MC steels are shown in Fig. 14.

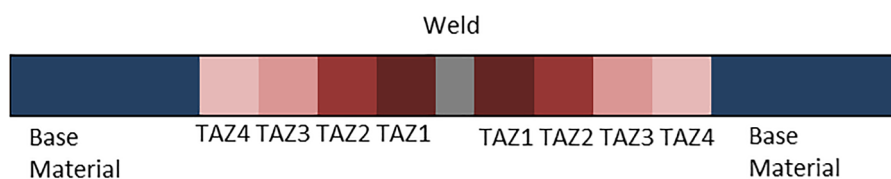


Fig. 4. Butt welding scheme including four TAZs.



Fig. 5. Vickers Matsuzawa MXT 50 microdurometer.



Fig. 6. Test samples used to perform Vickers hardness test.

4. Prediction of fatigue behavior of S235JR, S355MC, and S500MC steels depending on monotonic properties

The fatigue behavior of metallic materials is usually represented by the Wöhler curves [4] or S-N curves, which relate the load amplitude applied over the material, vs. the number of cycles that it holds until the final break. In the case of a high number of fatigue cycles, the properties that define the fatigue material behavior or number of reversals to failure, N_f , are the reversing stress σ_a , fatigue strength coefficient $\hat{\sigma}_f$, and fatigue strength exponent b , which appear in the Basquin's equation (5).

$$\sigma_a = \hat{\sigma}_f \cdot (N_f)^b \quad (1)$$

Based on this equation, there are a series of methods based on the monotonic properties for obtaining the fatigue behavior of steel, such as the Mischke method [6], SAE method [7], the linear logarithmic adjustment method explained by Besa and Giner [8], the method of Shigley [9], and the Juvinal method [10].

However, owing to the fact that the load cycles in the semitrailer are not alternating but fluctuating, the applied criteria were modified in order to consider the effect of the mean stress in the fatigue life prediction. This correction was introduced in the analysis by using the correction method developed by Morrow [11].

Morrow developed an approximation method to obtain the fatigue life prediction, applicable to any type of fatigue life prediction criterion, which obtained the fatigue life of a studied specimen considering the applied average stress. The method consists of replacing the fatigue life provided by any conventional criterion by a value obtained by means of the following expression:

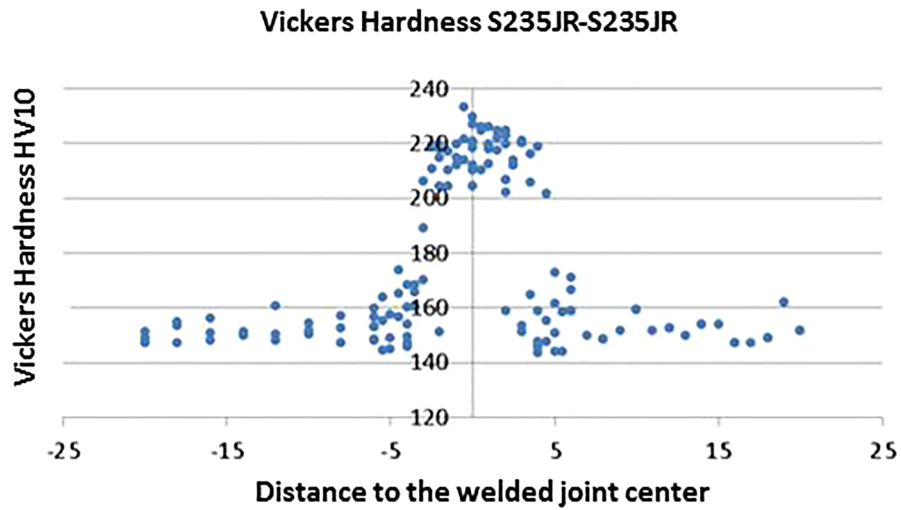


Fig. 7. Vickers hardness in welded specimens of S235JR.

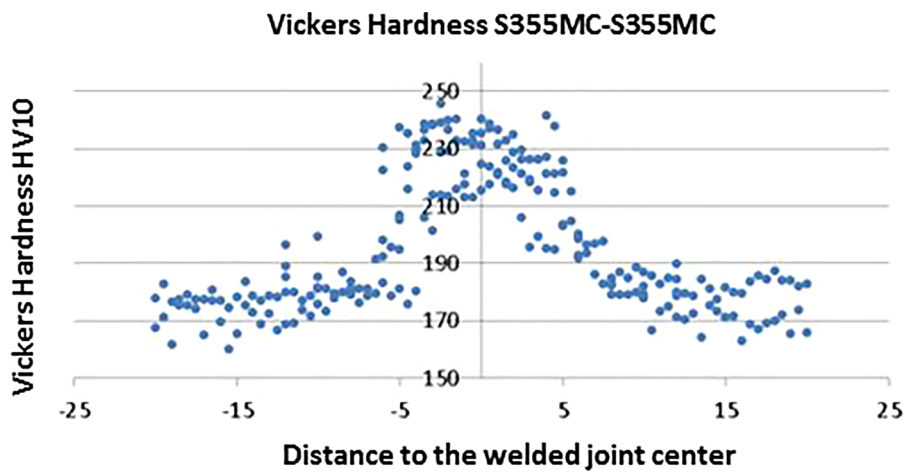


Fig. 8. Vickers hardness in specimens welded in steel S355MC.

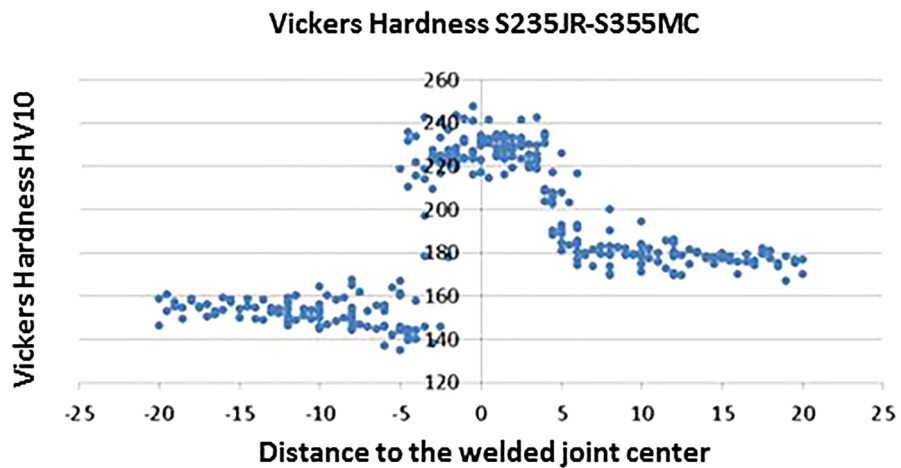


Fig. 9. Vickers hardness in welded specimens combining S235 JR-S355 MC steels.

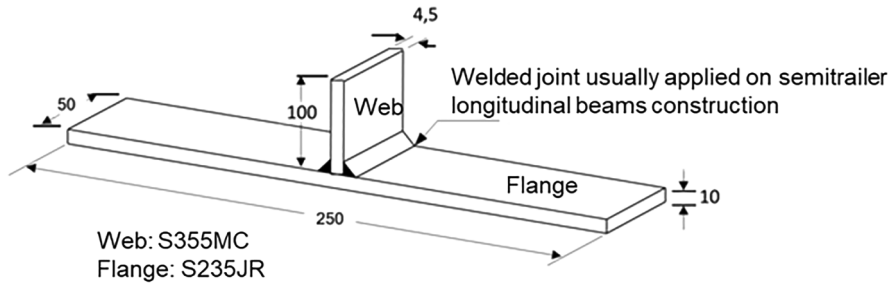


Fig. 10. Scheme of T-shaped welded specimens.

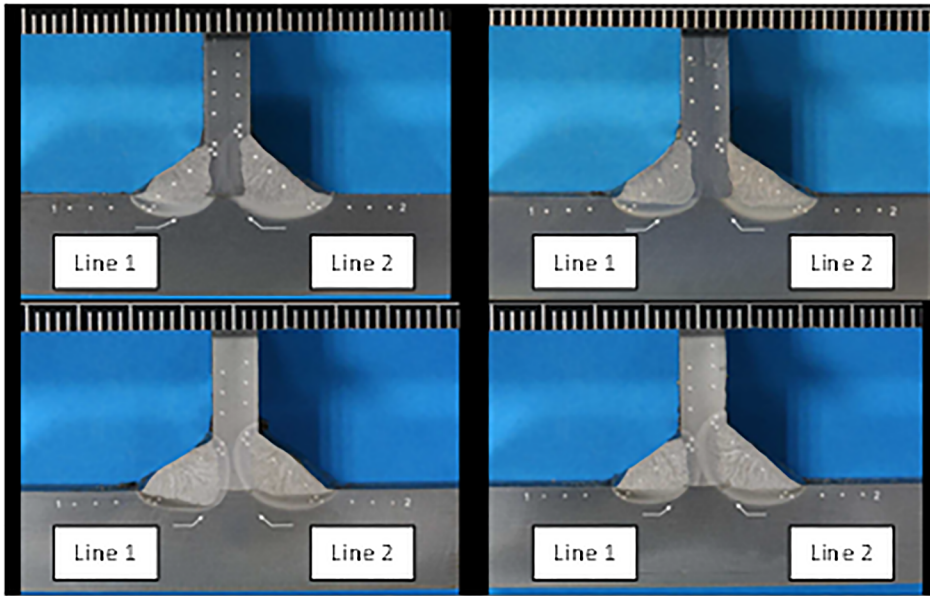


Fig. 11. Macrographs of T-shaped welded specimens.

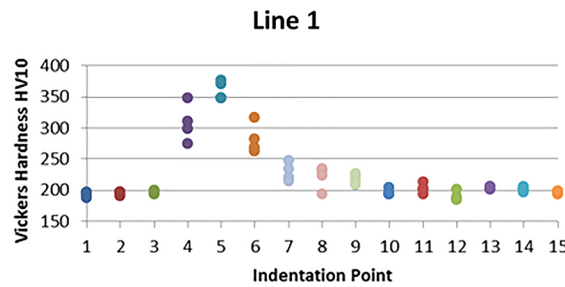


Fig. 12. Hardness test results in T-shaped welded specimens, Line 1.

$$N = N^* \cdot \left(1 - \frac{\sigma_m}{\sigma_f} \right)^{\frac{-1}{b}} \tag{2}$$

Therefore, once the number of reversals to failure is obtained for a given load case whose mean stress is zero, N^* , the number of cycles with the corrected mean stress N , can be obtained. σ_m is the average stress, σ_f is the fatigue strength, and b is the fatigue strength exponent.

In the bibliography, there are numerous criteria for fatigue life prediction in metallic materials. Some of these prediction criteria were based on different modifications of the Basquin-Manson [12]-Coffin [13] equation.

$$\frac{\Delta \epsilon}{2} = \frac{\sigma_f'}{E} \cdot (N_f')^b + \epsilon_f' \cdot (N_f')^c \tag{3}$$

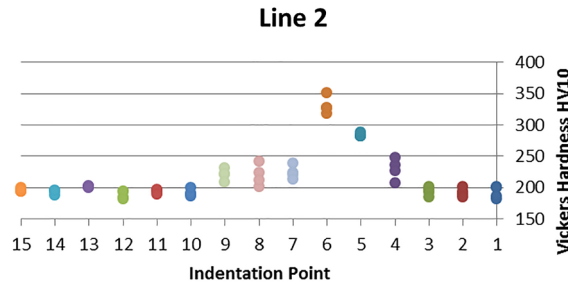


Fig. 13. Hardness test results in T-shaped welded specimens. Line 2.

Table 3
Mean hardness and equivalent strength.

	S235JR Base	TAZ S235JR	S355MC Base	TAZ DX355MC	S500MC Base	TAZ S500MC	Weld bead
Vickers Hardness HV10	194	299	199	194	217.5	208.2	222
Strength. (MPa)	620.5	961.75	636.75	620.5	697.5	668.35	711.5

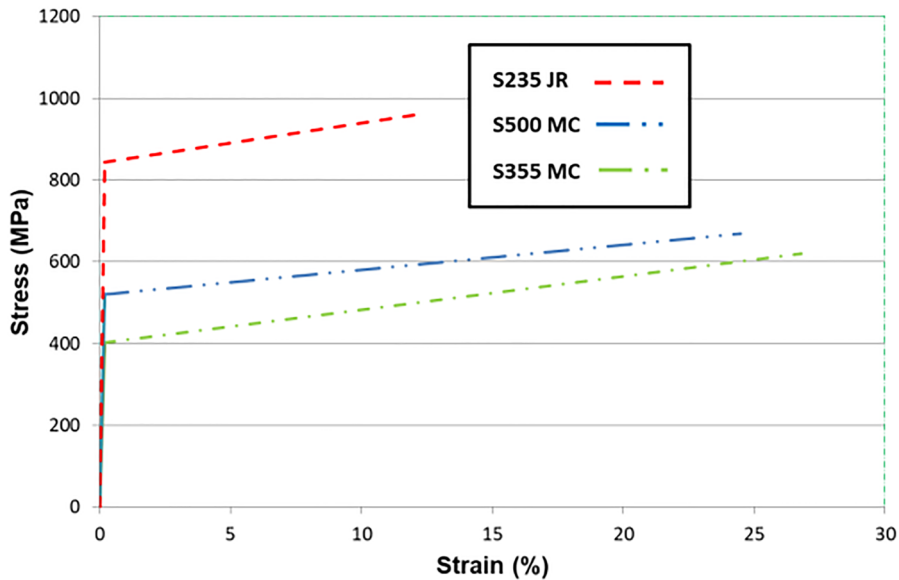


Fig. 14. Bilinear stress-strain curve for TAZs of S235JR, S355MC, and S500MC steels.

All criteria presented here have a common denominator: the fatigue parameters are collected from the monotonic properties obtained in tensile tests.

The tensile test is a totally uniaxial test. For this reason, the criteria explained in this section are considered criteria for predicting life to uniaxial fatigue loading.

The equations that relate the ultimate tensile strength, ductility, and Young’s modulus to the fatigue life for any range of strain were obtained through the experimental fatigue life characterization of 49 materials. These equations are the Universal Slope Method [14] and the four-point correlation (15). The fatigue parameters established by the modified universal slope method are those shown in the following equations:

$$\sigma'_f = E \cdot 0.623 \cdot \left(\frac{R_m}{E}\right)^{0.832} \tag{4}$$

$$b = -0.09 \tag{5}$$

$$\epsilon'_f = 0.0196 \cdot \epsilon_f^{0.155} \cdot \left(\frac{R_m}{E}\right)^{-0.53} \tag{6}$$

$$c = -0.56 \tag{7}$$

Table 4

Modified universal slope criterion fatigue properties of S235JR, S355MC, and S500MC steels.

Modified universal slope criterion						
	S235JR		S355MC		S500MC	
$\hat{\sigma}_f$ (MPa)	943.37		1039.85		1124.32	
E (MPa)	216,975	Exp.	217,193	Exp.	201,925	Exp.
R_m (MPa)	555.66	Exp.	624,52	Exp.	697.5	Exp.
b	-0.09		-0.09		-0.09	
ε_f	0,442		0.425		0,37	
e_f	0,741	Exp.	0,858	Exp.	0.67436	Exp.
c	-0.56		-0.56		-0.56	

where $\hat{\sigma}_f$ is the fatigue strength coefficient, E is Young's modulus, b is the fatigue strength exponent, ε_f is the fatigue ductility coefficient, e_f is the monotonic fracture ductility, c is the fatigue ductility exponent, and R_m is the ultimate tensile strength.

The fatigue properties listed in Table 4 were obtained by applying Eqs. (4)–(7) to the results obtained in the tensile tests for steels S235JR, S355MC, and S500MC.

5. Fatigue life prediction criterion for welded joints

Until now, different criteria and methodologies have been analyzed to make fatigue life predictions in base materials. However, the analysis that offers the best results for fatigue life in the Thermally Affected Zones by the welding process is that carried out by the International Welding Institute (IIW) [17,18], as stated Malon in his Doctoral Thesis [16].

The IIW establishes recommendations for the design and analysis of fatigue life in welded components owing to the modifications in the material properties that originate in the welding process [34].

The recommendations established by the IIW for fatigue life are valid for steels having a yield stress up to 960 MPa. In addition, these recommendations are not valid for low cycle fatigue, for cases in which the maximum working stress is higher than the material yield stress, or in cases where the temperature is high and there is a creep phenomenon [23].

Fig. 15 shows two different values of the Fatigue Stress Amplitude (FAT or “stress stroke”) that gives a fatigue life of two million cycles for steel overlap welded joints. A FAT parameter equal to 36 corresponds to failures occurring at the welding root or weld throat. A FAT parameter equal to 63 corresponds to failures occurring at the weld bead base or weld toe, just in the Thermally Affected Zone.

Although the International Institute of Welding recommends applying both FAT specifications, the experimental results carried out by the Department of Mechanical Engineering of the University of Zaragoza showed that for steels under study in this work, all breaks took place in the Thermally Affected Zone. Therefore, the value considered in this paper for the FAT parameter is 63.

The detail category for T-shaped welded joints stated by Eurocode 3 [35] is shown in Fig. 16).

It can be observed that for T-shaped welded joints whose flanges have a thickness lower than 50 mm and are independent of the web thickness have a detail category (FAT) equal to 80.

For the T-shaped welded specimens tested to perform this work, the failure occurred in the weld toe, as shown in Fig. 16. Therefore, the considered FAT value or detail category for the tested samples was also 80.

According to Eurocode 3, the S-N fatigue life curves have the following expression:

$$\log N = \log a - m \cdot \log \Delta \sigma, \quad (8)$$

where N represents the number of cycles or reversals to failure, m is the slope of the S-N curve, and $\Delta \sigma$, is the fatigue stress amplitude or stress stroke.

The $\log a$ value is obtained by solving Eq. (8) for 2 million cycles and where $\Delta \sigma$ represents the detail category for a slope $m = 3$. A slope of 3 is the value to consider for normal stresses, up to a number of cycles or reversals to failure, N , equal to 10^7 cycles. Until that N value, the m slope varies according to the application for which the fatigue life is being calculated. For N greater than 10^7 cycles, the m slope is null.

Table 5 lists $\log a$ values calculated for each of the joining typologies presented in this work, which are the overlap welded joint and the T-shaped welded joint.

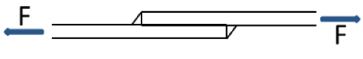
	
Description:	FAT
Transverse loaded overlap joint with fillet welds:	
Stress in plane weld toe (toe crack)	63
Stress in plane weld throat (root crack)	36

Fig. 15. FAT class in IIW equivalent to “detail category” in Eurocode of overlapping welded joints.

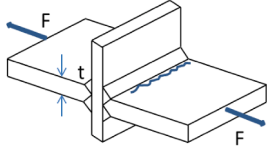
	Description: T-shaped welded joint. Full penetration. Toe failure. $t < 50$ mm	FAT 80
---	---	------------------

Fig. 16. Detail category of T-shaped welded joints.

Table 5

S-N curve parameters according to IIW criteria.

Joint type	Detail Category	$\log(\Delta\sigma_r)$	N	$\log N$	m	$\log a$
Overlap	63	1.7993	$2 \cdot 10^6$	6.301	3	11.699
T-shaped	80	1.9031	$2 \cdot 10^6$	6.301	3	12.010

6. Experimental characterization of fatigue properties of the S235JR, S355MCD, and S500MC

Fatigue tests were carried out on overlap-welded samples under alternating or fluctuating load conditions. The aim was to obtain the survival probability distribution for the different load cases and to verify that the results were adjusted to a Weibull distribution to determine the fatigue life. S235JR, S355MC, and S500MC steel specimens were tested, and mixed specimens joining two different steels were also manufactured and tested Fig. 17.

The failure for the S235JR, S355MC, and S500MC specimens and mixed tested specimens always occurred in the Thermally Affected Zone closest to the weld bead, or TAZ1, as seen in Fig. 18.

The results obtained in the fatigue tests, with different levels of mean load and load amplitude for the overlapping specimens of S235JR, are summarized in Table 6.

7. Weibull distribution

The probability density function of the Weibull [20,21] distribution is as follows:

$$f(t) = \frac{\beta}{\alpha^\beta} t^{\beta-1} e^{-\left(\frac{t}{\alpha}\right)^\beta}, t > 0 \quad (9)$$

where α and β are positive parameters, α is the scale parameter, and β is the form or profile parameter. Fig. 19 shows the form of different reliability functions of the Weibull distribution for a value of parameter $\alpha = 1$ and different values for parameter β . Later, this parameter β will be referred to the number of cycles.

The next step was to verify if the fatigue experimental data fit a Weibull distribution. For this purpose, the graph $\ln(\ln(1/R_n(t)))$ vs. $\ln(t)$ was charted, where t is the data along the x-axis, and $R_n(t)$ is the empirical reliability function.

The implementation of the Weibull probabilistic distribution chart uses the following steps:

- Sort the results of the life cycles from lowest to highest

$$t_1 \leq \dots \leq t_i \leq \dots \leq t_n \quad (10)$$

- Assign ranges
- Calculate $F_n(i)$, which represents the percentage of failures that occur before the time corresponding to range i . The calculation of this parameter depends on the authors. In this case, the Herd-Johnson method according to Nelson [22] is used:

$$F_n(i) = \frac{i}{(n+1)} \quad (11)$$

- Finally, the points are drawn. For the rank of i failure, $\ln(t(i))$ is placed in the abscissas, and $\ln(\ln(1/(1-F_n(i))))$ is located on the ordinate axis.



Fig. 17. Overlap-welded samples.



Fig. 18. Overlap-welded samples after fatigue failure.

Table 6

Fatigue results in overlap-welded specimens S235JR–S235JR.

S235JR-S235JR			
Test sample	Mean load (kN)	Amplitude load (kN)	Number of cycles to failure
1	22	18	60
2	20	10	91,090
3	20	10	84,893
4	20	10	58,594
5	20	10	92,872
6	16	14	16,580
7	16	14	26,882
8	16	14	20,410
9	20	5	477,985
10	20	15	33,181
11	20	15	17,360
12	20	15	26,739
13	25	5	574,794
14	25	5	782,160
15	25	5	402,728
16	18	12	38,472
17	18	12	41,127
18	18	12	34,465
19	25	5	1,671,200

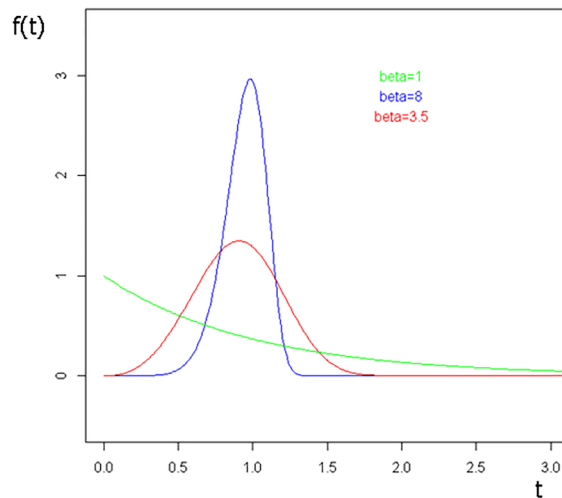


Fig. 19. Density function of Weibull distribution for different values of β and $\alpha = 1$.

- On this basis, it can be visually determined if the data matches a line. Moreover, a least-squares adjustment can be used.

The results obtained for each load case were evaluated. For example, the results obtained for steel S235JR overlap-welded specimens with an average load of 25 kN and amplitude of 5 kN are shown in Fig. 20.

The results in terms of the Weibull adjustment were obtained for different average loads and amplitudes for the three studied steels. Afterward, the real mean load to which the test samples were subjected was corrected by the Morrow equation. Thus, the equivalent number of cycles was obtained, corresponding to the equivalent load, related to the equivalent load amplitude and a null mean load.

As an example of the data, the results of the Weibull adjustment and Morrow correction for a 5 kN load amplitude and S235JR steel overlap-welded specimens are shown in Fig. 21.

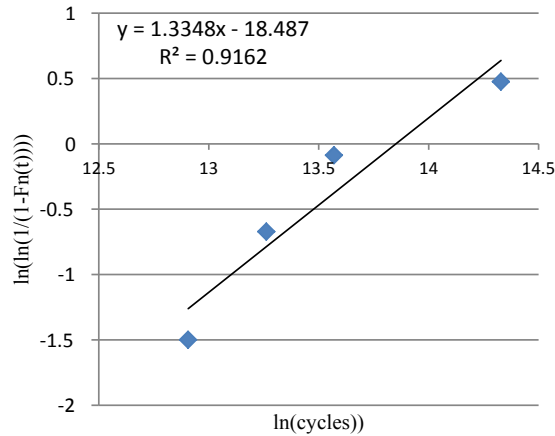


Fig. 20. Weibull adjustment for Steel S235JR overlap-welded samples. Average Load = 25 kN. Amplitude = 5 kN.

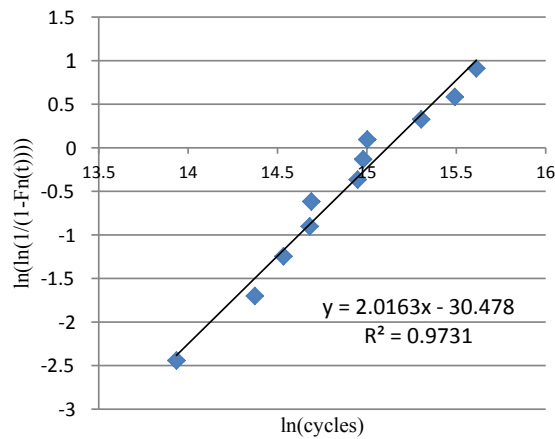


Fig. 21. Weibull adjustment for steel S235JR overlap-welded samples. Amplitude = 5 kN (Morrow correction).

8. Adjustment by using R-software of data distribution obtained by testing of overlap-welded specimens

The R-software [23] includes different analysis packages to check if a testing data series fits a probability distribution. The package that has to be loaded to perform the operations detailed here is the MASS package [36].

The first function of this package to be used is the “fitdistr ()” function, which estimates the parameters of a distribution by the maximum likelihood method [24]. In this case, the parameters that were being estimated were those of a two-parameter Weibull distribution: the shape parameter and the scale parameter.

“fitdistr ()” function needs to pass at least two arguments. The first argument is the data vector that represents the number of cycles to fatigue failure, and the second argument is the distribution type for which it is wanted to calculate the parameters according to the maximum likelihood method.

Once the Weibull distributions that best fit the data obtained from experimental fatigue testing are obtained, it is necessary to check the accuracy of this adjustment. To do so, the following contrast of hypotheses is proposed:

H_0 : The data sample fits the given distribution

H_1 : The data sample does not fit the given distribution

There are different tests in the bibliography to carry out the verification of the adjustment accuracy. Some of them are the chi-square test proposed by Karl Pearson [26], the Kolmogorov-Smirnov [27] test, and a test by Anderson-Darling [25].

The test applied in this study was the Anderson-Darling test since it has been shown to offer better results in terms of fit accuracy for small-sized batches of samples such as those studied in this analysis, as stated in Mohd and Bee [37].

The Anderson-Darling test is based on the differences between a distribution function $FO(t)$ and the empirical distribution function, where the empirical estimator of the distribution function is the following, as confirmed by Kalbeish and Prentice [38]:

$$\hat{F}(t) = \frac{\text{Number of observations } \leq t}{n} \tag{12}$$

The statistic of this test is

Table 7

Weibull distribution parameters, Anderson-Darling test, and p-value for S235JR and S355MC steel specimens.

Steel	Load	Weibull Parameter			Anderson-Darling	p-value
		Shape	Scale			
S235 JR	5	2.3707	3.629×10^6		0.2611	0.964
	10	3.3949	3.52×10^5		0.6118	0.6321
	12	1.7329	1.65×10^5		0.2641	0.9689
	14	5.6387	8.28×10^4		0.2943	0.945
	15	2.2485	1.18×10^5		0.6667	0.5831
S355 MC	5	2.2524	9.10×10^6		0.9931	0.3591
	10	9.3035	4.93×10^5		0.42445	0.821
	12	4.8440	2.06×10^5		0.5848	0.6562
	14	29.377	7.44×10^4		0.3619	0.8813
	15	7.5735	1.64×10^5		0.4879	0.755

$$A_n^2 = \int_{-\infty}^{\infty} \frac{(\hat{F}(t) - F_0(t))^2}{F_0(t)(1 - F_0(t))} dF_0(t) \quad (13)$$

Critical values are tabulated and the null hypothesis H_0 is rejected for large values of the statistic A_n^2 [39].

The ADGof Test package in the R-software, explained by Gil [40], is able to perform the Anderson-Darling test to check if the data fit accurately to a Weibull distribution.

The p -value is considered a measure of the statistical evidence provided by the data in favor of the alternative hypothesis H_1 (or against H_0). When the p -value is lower or equal to 0.05, there is strong evidence in favor of H_1 .

For illustrative purposes, the Weibull distribution parameters, Anderson-Darling test, and p -value are shown in Table 7 for the S235JR and S355MC steel specimens and for different load amplitudes.

9. Modification of fatigue life prediction curves of IIW based on specific parameters of material: Tello-Castejon adjustment model

Based on the fatigue life prediction criteria of the IIW, different modifications were made to obtain better results, taking into account the base material parameters before welding and the material properties of the Thermally Affected Zones after the welding process.

The scheme followed to obtain the new fatigue life prediction criterion in welded joints is shown in Fig. 22.

First, fatigue tests were carried out on overlap-welded samples under alternating or fluctuating load conditions in order to obtain the corresponding fatigue characterization. Second, the results were transformed to equivalent results with null mean loads by means of the Morrow equation.

Subsequently, fatigue results were represented in an S-N chart, and the fatigue life prediction curve established by the IIW was also represented for the corresponding geometry when selecting the adequate FAT (detail category). Both curves were compared, and the difference in the stress stroke and the difference in the slope between both curves were determined.

Figs. 23–25 show the fatigue life testing curves of the overlap-welded specimens for different steels, transformed by the Morrow equation for a null mean load. Having obtained the difference between the fatigue experimental curves and the fatigue IIW curves in terms of the stress stroke and variation of the slope, the following properties were also needed: the base material mechanical properties and the mechanical properties of the Thermally Affected Zones. Subsequently, fatigue life prediction curves were obtained for the materials studied, as it explained later. The studied steels, namely, S235JR, S355MC, and S500MC, are typically applied in semi-trailer construction.

The following expressions were obtained for the S-N curves:

$$\text{S235JR: } y = 8220.3 \cdot x^{-0.294} \quad (14)$$

$$\text{S355MC: } y = 2616.5 \cdot x^{-0.199} \quad (15)$$

$$\text{S500MC: } y = 3082.7 \cdot x^{-0.189} \quad (16)$$

where y is the Stress stroke, and x is the number of cycles.

The exponents of the curves obtained for the studied steels are listed in Table 8. In addition, the quotient (Lelast_base/RmTAZ) was obtained by dividing between the base material yield stress (Lelast_base) and the strength of the Thermally Affected Zone (RmTAZ). These results are listed in Table 8 for the tested steels.

It can be observed in Table 8 that as the quotient between the base material yield stress (Lelast_base) and the strength of the Thermally Affected Zone (RmTAZ) increases, a decrease in the exponent of the S-N fatigue life transformed curves for a null mean load takes place.

It can be deduced that the relationship between these two parameters follows the equation shown below, with an R^2 adjustment of 0.9724:

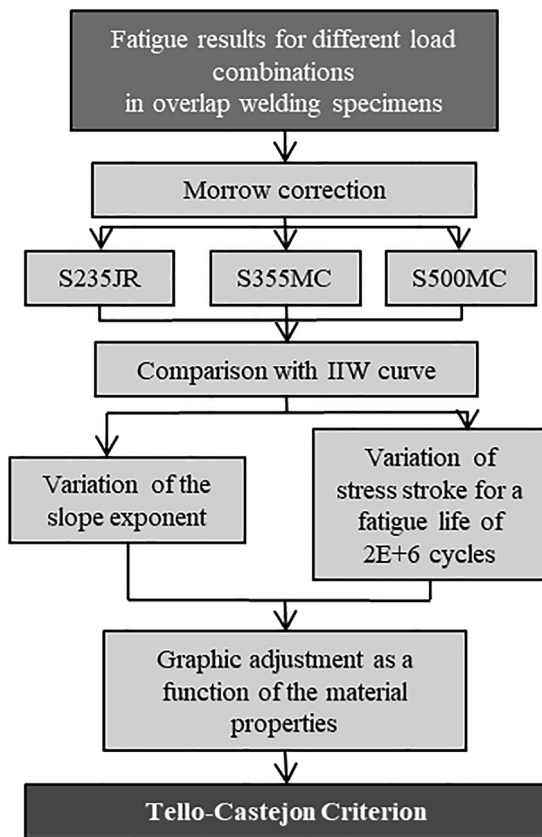


Fig. 22. Diagram for obtaining Tello-Castejon criterion.

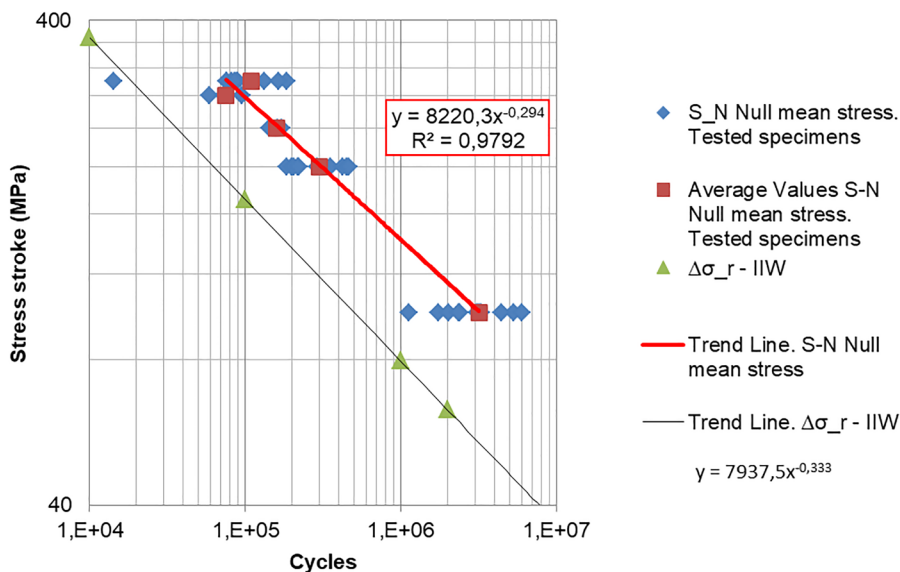


Fig. 23. Fatigue life transformed curves of overlap-welded samples for steel S235JR.

$$\left(\frac{L_{elast_{base}}}{R_{mTAZ}}\right) = 0.0254 \cdot (Exponent)^{-2.066} \tag{17}$$

This expression has been called the first equation of the Tello-Castejon criterion for the adjustment of the exponent of a fatigue life curve slope in welded joints. By means of the base material yield stress and the strength of the Thermally Affected Zone for a specific

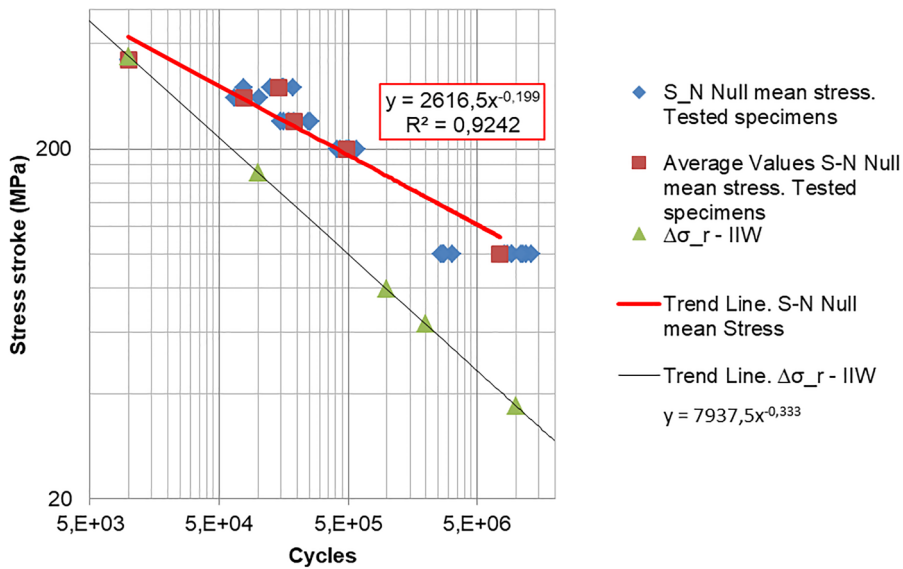


Fig. 24. Fatigue life transformed curves of overlap-welded samples for steel S355MC.

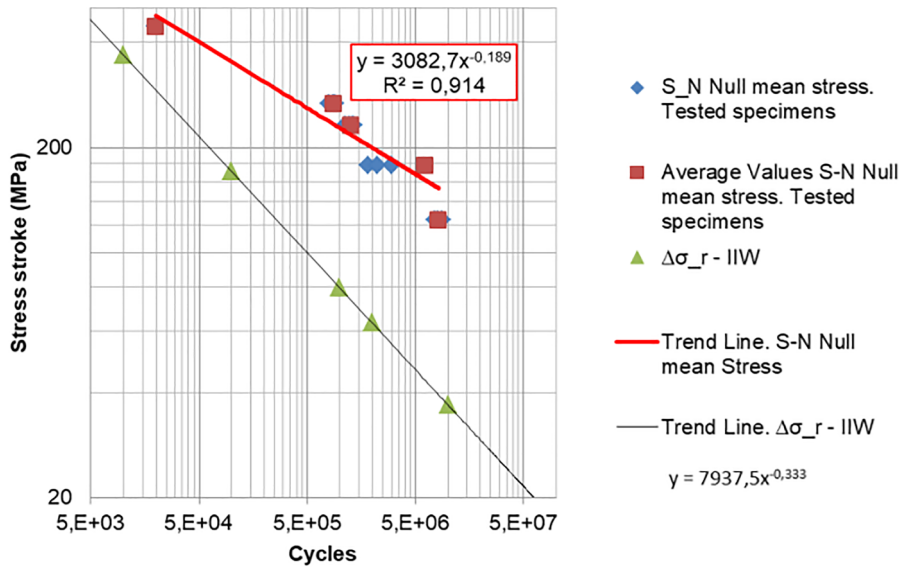


Fig. 25. Fatigue life transformed curves of overlap welded samples for steel S500MC.

Table 8

Slope of fatigue life prediction curves as stated by IIW and experimentally obtained for tested steels.

Slope variation justification				
	IIW	S235JR	S355MC	S500MC
Exponent	0.333	0.294	0.199	0.189
Yield stress of the base steel (Lelast_base) (MPa)		309.73	405.27	574.11
RmTAZ (MPa)		961.75	620.5	668.35
(Lelast_base/RmTAZ)	-	0.322	0.653	0.859

steel, and with the application of this equation, it is possible to obtain the exponent of the fatigue life transformed curve for a null mean load, related to the steel considered.

The IIW criterion for adjusting the fatigue curve establishes a stress stroke for a fatigue life of 2×10^6 cycles that varies depending on the joint geometry, which is called the detail category or FAT. For the case of the overlap-welded specimens, the detail category

Table 9

Variation of stress stroke with respect to IIW.

Cut point variation justification				
	IIW	S235JR	S355MC	S500MC
Stress stroke for 2×10^6 cycles (MPa)	63	115.45	145.82	198.63
1000/Stress stroke increment	–	19.067	12.074	7.373
(Lelast_base/Rmzt)	–	0.322	0.653	0.859

established by the IIW is 63, which is the value of the tension stroke in MPa that corresponds to a fatigue life of 2×10^6 cycles.

Table 9 lists the experimental fatigue results obtained for the tested steels. The stress stroke value at 2×10^6 cycles established by the IIW criterion corresponds to a 95% survival probability. However, values listed in Table 9 for the tested steels correspond to a stress stroke of the average number of survival cycles, which is 50%. Therefore, the stress stroke increment is the stress stroke for 2×10^6 cycles, obtained for each steel, minus 63 MPa.

It can be observed in Table 9 that as the quotient between the base material yield stress (Lelast_base) and the strength of the Thermally Affected Zone (RmTAZ) increases, a decrease in the 1000/stress stroke increment expression takes place.

It can be deduced that the relationship between these two parameters follows the equation shown below:

$$\left(\frac{\text{Lelast}_{\text{base}}}{\text{RmTAZ}}\right) = -0.046 \cdot \left(\frac{1000}{\text{Stress stroke increment}}\right) + 1.2022 \quad (18)$$

This expression has been called the second equation of the Tello-Castejon criterion for the adjustment of the stress stroke increment compared with that of the IIW. By means of the base material yield stress and the strength of the Thermally Affected Zone for a specific steel, and with the application of this equation, it is possible to obtain the stress stroke of the fatigue life transformed curve for a null mean load, related to the steel considered.

The Tello-Castejon criterion can be considered the most important contribution from this paper, given that for a commonly used steel in semi-trailer manufacturing with a usual yield stress between 260 and 960 MPa, it allows for the estimation of the corresponding fatigue life transformed curve for a null mean load. The only parameters needed for that estimation are the base material yield stress and the strength of the Thermally Affected Zone. Furthermore, the obtained fatigue life curve can be applied to the calculation of the fatigue life of a semi-trailer and its components or other structures with a determined survival probability according to the Weibull distribution.

The amount of work involved in obtaining each curve such as those presented in Eqs. (14)–(16) for each combination of welded steels applied on welded semi-trailer components is very high. However, it is relatively easy to experimentally obtain the yield stress of a base steel, if this value it is not given by the steel producer, and RmTAZ by conducting hardness testing. These two parameters alone are sufficient to define the equation that relates the stress stroke ($\Delta\sigma_r$), and the number of cycles (N) by means of the Tello–Castejon criterion, as follows:

1. Acquisition of the yield stress of a determined steel ($\text{Lelast}_{\text{base}}$) and the strength of its RmTAZ.
2. Calculation of the quotient ($\text{Lelast}_{\text{base}}/\text{RmTAZ}$)
3. Determination of the corresponding S–N curve: $\Delta\sigma_r = \text{Coefficient} \cdot N^{(-\text{Exponent})}$

3.1 where the Exponent can be obtained from the first equation of the Tello–Castejon criterion:

$$\left(\frac{\text{Lelast}_{\text{base}}}{\text{RmTAZ}}\right) = 0.0254 \cdot (\text{Exponent})^{-2.066}$$

$$(\text{Exponent}) = \left\{ \frac{1}{0.0254} \left(\frac{\text{Lelast}_{\text{base}}}{\text{RmTAZ}} \right) \right\}^{\left(\frac{1}{-2.066}\right)} = \left\{ 39.37 \left(\frac{\text{Lelast}_{\text{base}}}{\text{RmTAZ}} \right) \right\}^{-0.484}$$

3.2 and the Coefficient can be obtained from the second equation of the Tello–Castejon criterion:

$$\left(\frac{\text{Lelast}_{\text{base}}}{\text{RmTAZ}}\right) = -0.046 \cdot \left(\frac{1000}{\text{Stressstrokeincrement}}\right) + 1.2022$$

$$\text{Stress stroke increment} = \left(\frac{1000}{-0.046 \left\{ \left(\frac{\text{Lelast}_{\text{base}}}{\text{RmTAZ}} \right) - 1.2022 \right\}} \right) = \left(\frac{1000}{-21.74 \left\{ \left(\frac{\text{Lelast}_{\text{base}}}{\text{RmTAZ}} \right) - 1.2022 \right\}} \right)$$

$$\Delta\sigma_r = \text{Stress stroke} = \text{Stress stroke increment} + 63$$

$$\text{Coefficient} = \frac{2 \cdot 10^6 \cdot \text{Exponent}}{\Delta\sigma_r}$$

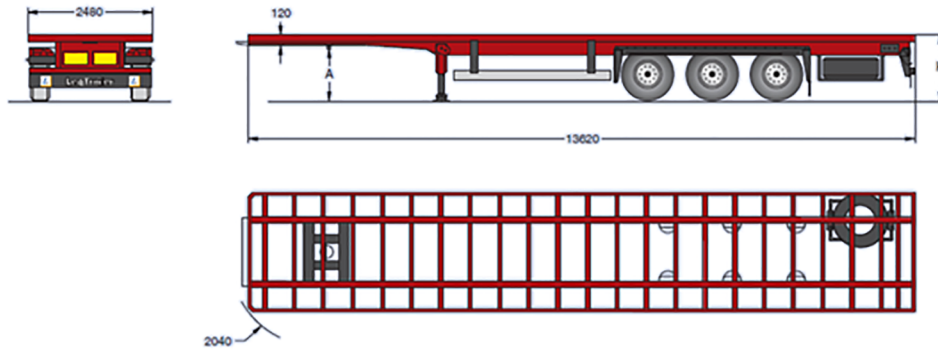


Fig. 26. Outline of three-axle semi-trailer from Lecitrailer.

By means of this procedure, the fatigue life testing curve of the overlap-welded specimens can be estimated for a particular steel with a usual yield stress between 260 and 960 MPa, such as those generically applied in the semi-trailer industry, transformed by the Morrow equation for a null mean load.

Therefore, this procedure is intended to be particularly useful for steels that do not have a complete characterization of their fatigue parameters.

Moreover, fatigue life testing curves obtained in this way can be incorporated into a post-process subroutine to determine the fatigue life of welded components of semi-trailers, particularly in their TAZs, as a function of the survival probability, as will be shown in the following chapter.

10. Numerical and experimental analysis of a three-axle semi-trailer bracing support

Three-axle semi-trailer vehicles are characterized by the fact that the front part of the structure is supported on the fifth wheel of the tractor cabin by means of a King Pin. Fig. 26 shows a three-axle platform semi-trailer.

At the rear of the semi-trailer structure, the three axles are mounted on the bracing supports. The axle bracing assembly is formed by the axle bracing support, the shaft, and the air spring. Fig. 27 shows a bracing support-shaft-air spring assembly of a three-axle semi-trailer.

Two different configurations of axle bracing support were tested and calculated. As can be seen in Fig. 28, the axle bracing supports on which the shaft is underpinned in the assembly are different. These axle bracing supports are called a straight-shaped support and curved-shaped support in order to differentiate them. Calculations and testing were carried out with this assembly. Therefore, it was possible to verify which had a higher strength and a longer fatigue life.

11. Calculation by means of finite element method of axle bracing support of a three-axle semi-trailer

Initially, a finite element model of the subassembly [41,42] was developed to conduct a numerical analysis of the two axle bracing supports. A total of 42,350 elements and 42,100 nodes were applied to the numerical model. The elements used for modeling the subset are linear shell type. The type of analysis was linear static and the maximum load was applied. An image of the first complete subset model is shown in Fig. 29.

The curve-shaped support and straight-shaped support are shown in Fig. 30. Moreover, it can be seen how Thermally Affected



Fig. 27. Support-shaft-air spring assembly for semi-trailer.

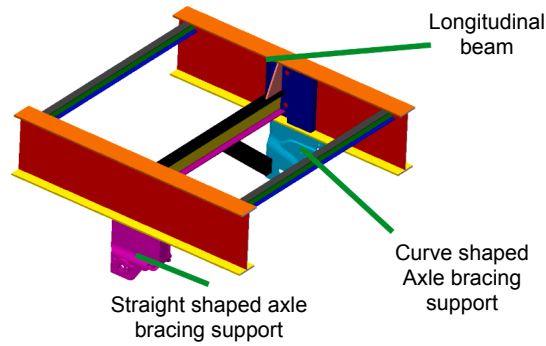


Fig. 28. Exploded view of bracing support assembly.

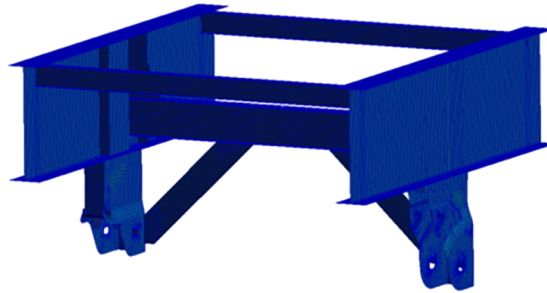


Fig. 29. Finite element model of axle bracing assembly.

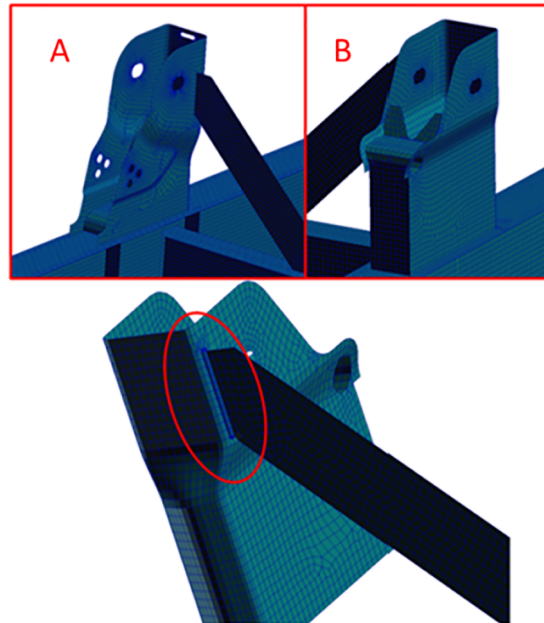


Fig. 30. Detail of two different axle bracing supports: curve-shaped (A) and straight-shaped (B).

Zones were modeled in the junction area of the diagonal reinforcements with the axle bracing support.

Calculations and tests were carried out for the entire assembly. First, a numerical analysis was developed for the bracing support assembly including the two different axle bracing supports. The loads applied to the finite element model are shown in Fig. 31. A lateral alternating sine wave load with a 3.5-T amplitude and null average load was applied to each support. This lateral load took place in the first and third axes of the semi-trailer when a minimum radius turn maneuver was being driven. Fig. 32 shows the von Mises (MPa) stress distribution obtained by applying 3.5-T loads to each support pin.

The fatigue life of the axle bracing assembly was calculated by executing the fatigue life prediction procedure explained in this

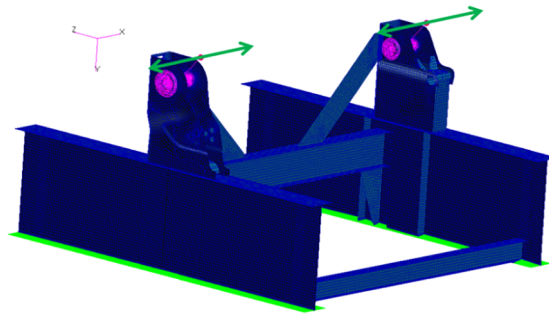


Fig. 31. Loads applied over axle bracing assembly.

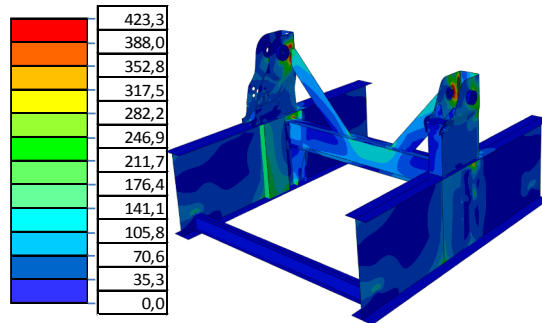


Fig. 32. Von Mises stresses when applying 3.5-T loads.

article, considering the application of the load case previously explained. A 50% and a 95% survival probability were considered.

Figs. 33 and 34 show the results of the fatigue life prediction for this 3.5-T load case and for 50% and 95% survival probabilities. These results focused on the most unfavorable support, which is the curve-shaped support.

Simultaneously, a fatigue test was carried out on a semi-trailer axle bracing assembly until the failure of a component took place. A curve-shaped support (type A) and straight-shaped support (type B) were welded to the subset. Loads were applied to both supports in a synchronized manner. Additionally, strain measurements were taken by means of an extensometric strain gauge rosette located in the curve-shaped support in order to measure the strain evolution along the test.

Fig. 35 shows the two supports that were tested under a lateral alternating sine-wave load of 3.5 T.

The extensometric strain gauge rosette was located on the side of the curved support. The detail of the rosette location can be seen in Fig. 36.

The axle bracing subset was rigidly attached to a metallic bench to carry out the fatigue test. The assembly of the bench and hydraulic actuator cylinders can be seen in Fig. 37.

The axle bracing assembly including two different axle bracing supports was tested under the conditions referred in Table 10.

The results of the test showed that at 640 cycles, there was a noticeable variation in the structure displacement owing to the

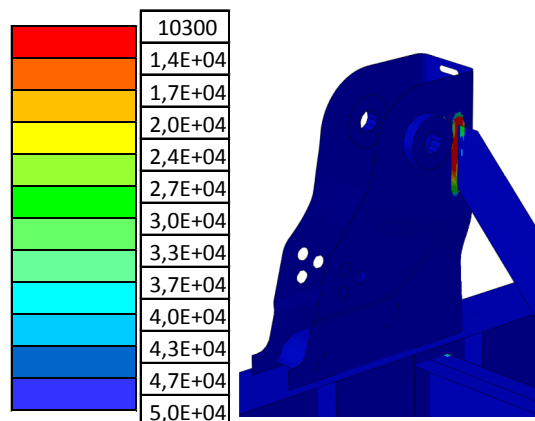


Fig. 33. Fatigue life prediction for 3.5-T load case and 50% survival probability for curve-shaped support.

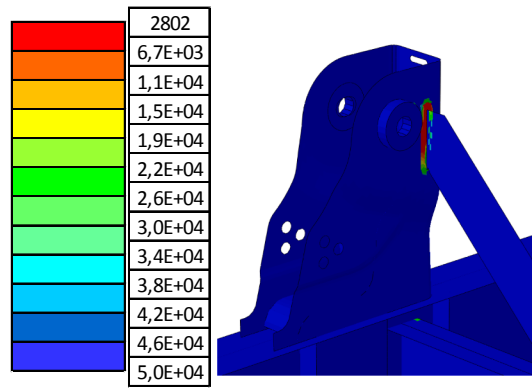


Fig. 34. Fatigue life prediction for 3.5-T load case and 95% survival probability for curve-shaped support.

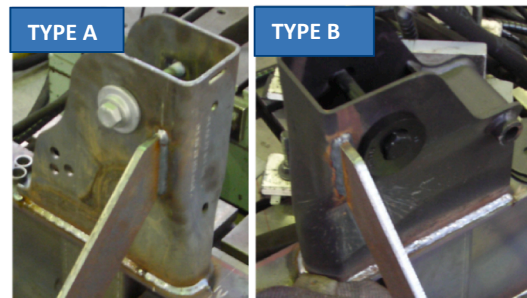


Fig. 35. Curve-shaped (Type A) and straight-shaped (type B) axle bracing supports in testing assembly.

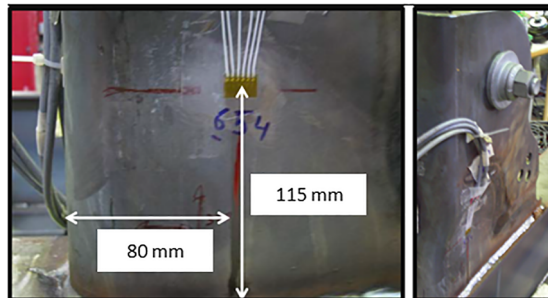


Fig. 36. Detail of strain gauge rosette location over curve-shaped support (type A).

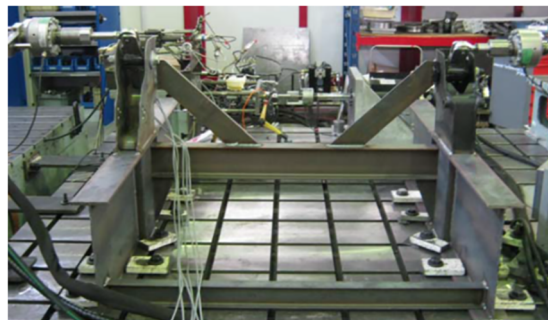


Fig. 37. Axle bracing assembly on test bench.

appearance of cracks in the joining areas of the axle bracing supports with the diagonal reinforcements.

Cracks appeared in both axle bracing supports. However, cracks in the curve-shaped bracing support (type A) were more apparent than those in the straight-shaped bracing support, to the point that cracks in the latter were not visible to the naked eye Fig. 38.

Table 10
Initial test conditions applied to axle bracing assembly and result in terms of fatigue life.

Temperature (°C)	23 (-5, +5)	Cylinders	INSTRON
Wave type	Sine	Load cell	INSTRON 50 kN
Control	By Load	Load (Tons)	-3.5/3.5
Frequency (Hz)	0.15	Cycles	640

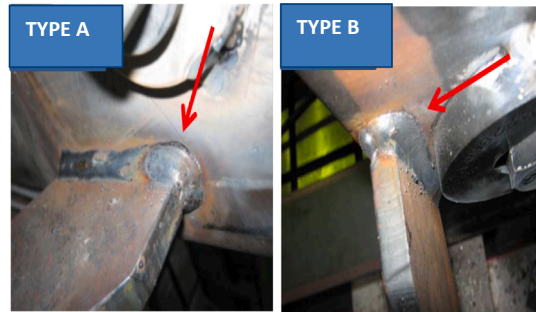


Fig. 38. Cracks in both axle bracing supports after 3.5-T load fatigue test.

The results obtained from the strain gauge rosette located on the curve-shaped bracing support (type A) are shown in Fig. 39. The scale of main stress 1 is shown on the left y-axis, whereas the scale of main stress 2 is shown on the right y-axis. Key stress values that were compared with the corresponding numerical ones are indicated with arrows in Fig. 39.

Equivalent von Mises stresses were obtained for the two ends of the 3.5-T load fatigue test from the results shown in Fig. 39. These are listed in Table 13.

Additionally, the elements of the finite element model that correspond to the position of the strain gauge rosette in the experimentally tested assembly were selected in order to correlate the experimental results with the numerical ones in terms of stress. Fig. 40 shows the elements that correspond to the strain gauge rosette placed in the curve-shaped support (type A).

The von Mises stresses obtained by FEM in these elements were 90.1 MPa for + 3.5 T of load and 89.35 MPa for - 3.5 T of load Fig. 41. The corresponding von Mises stresses experimentally obtained for the same loads were, respectively, 91.7 MPa and 83.5 MPa. Therefore, there was a numerical-experimental correlation greater than 93.5%.

Once testing of the bracing assembly with different supports was finished, a new axle bracing assembly was manufactured, in

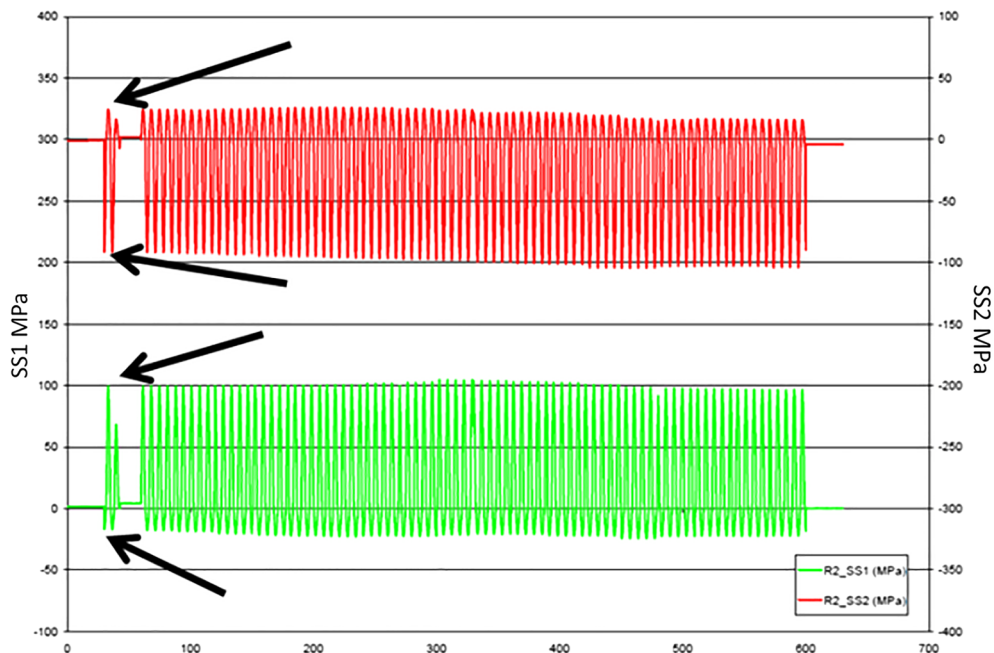


Fig. 39. Rosette measurements in 3.5-T load fatigue test.

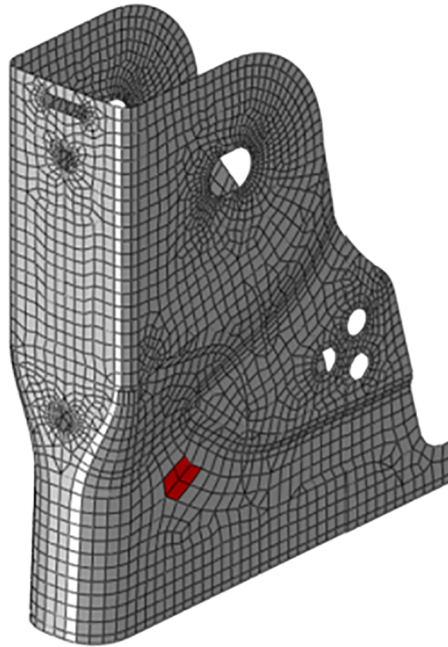


Fig. 40. Elements of finite element model of curve-shaped support (type A) at strain gauge rosette location.

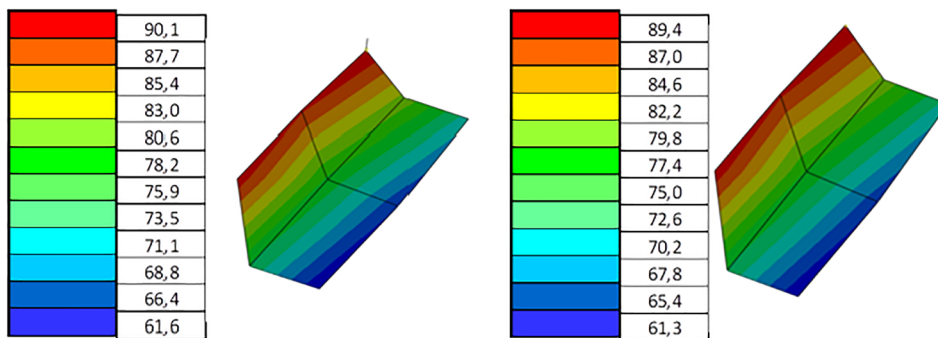


Fig. 41. Von Mises stress numerically obtained at strain gauge rosette. Left: +3.5-T load, right: -3.5-T load.

which both of the mounted supports were type B. The type B support exhibited the greatest fatigue resistance in the first test. Additionally, the test load was also reduced to 3-T to obtain a longer fatigue life. The new bracing assembly including both type B supports mounted on the test bed can be observed in Fig. 42.

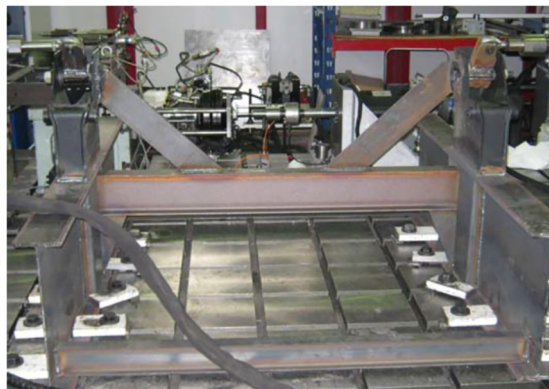


Fig. 42. New axle bracing assembly on test bench.

Table 11

New test conditions applied to new axle bracing assembly and result in terms of fatigue life.

Temperature (°C)	23 (−5, +5)	Cylinders	INSTRON
Wave type	Sine	Load cell	INSTRON 50 kN
Control	By Load	Load (Tons)	−3/3
Frequency (Hz)	0.15	Cycles	14,645

Conditions for conducting the 3-T test with the new axle bracing assembly, as well as the results obtained, are listed in Table 11.

Fig. 43 shows a detail of the crack produced in the axle support during the 3-T load fatigue test.

Fig. 44 shows the von Mises (MPa) stress distribution obtained by applying 3-T loads to each support pin of the new axle bracing assembly, in which two straight-shaped supports were included.

Figs. 45 and 46 show the results of the fatigue life prediction for this 3-T load case applied to the new axle bracing assembly and the results for 50% and 95% survival probabilities. In this bracing assembly both supports are type B or straight-shaped, given that this type exhibited a higher resistance in the previous test.

A summary of fatigue life results obtained numerically and experimentally is shown in Table 12.

For the second of the axle bracing assemblies tested under 3-T loads, the predicted fatigue life numerically obtained for a 50% survival probability is verified to be very well correlated with the experimental one.

12. Conclusions

The main contributions of this work are summarized below and can be used in the semi-trailer optimization process or any other kind of structure in general, by means of carrying out a fatigue analysis and its effect on the welded joints and structural components of this type of vehicle.

- Fatigue life characterization for different types of welded joints and for different combinations of widely used steels in semi-trailer manufacturing, such as S235JR, S355MC, and S500MC, was carried out.
- A fatigue life prediction criterion was developed for welded joints that takes into account the geometry of the welded joint as well as the mechanical properties of the base material and its Thermally Affected Zone (TAZ) after the welding process.
- By means of both equations of the Tello-Castejon criterion, it is possible to adjust the exponent and the variation of the stress stroke compared with the IIW, corresponding to the fatigue life transformed curve for a null mean load, related to the steel considered in welded joints. This procedure is especially useful for steels that do not have a complete characterization of their fatigue parameters.
- This fatigue life prediction criterion was implemented in a post-process subroutine to determine the fatigue life of welded components of semi-trailers, specifically in their Thermally Affected Zones. Moreover, the study focused on the joining between the axle bracing support and diagonal reinforcements and longitudinal beams.
- The methodology developed to predict the fatigue life in welded joints by using the Finite Element Method, and the developed fatigue life prediction criterion, were validated through the testing and simulation of a two semi-trailer axle bracing subset. A good correlation between numerical and experimental results was obtained when the fatigue life was significantly high. On the one hand, it has been verified that the fatigue life prediction criterion for welded joints, based on the work of the IIW, is not valid for very low cycle fatigue. On the other hand, considering that the fatigue life range of these subsets, which is traditionally approximately 15,000–20,000 before maximum load (minimum radio maneuver), a good correlation has been proven with the second tested subassembly.



Fig. 43. Detail of the crack in one of the axle bracing supports after a 3-T load fatigue test.

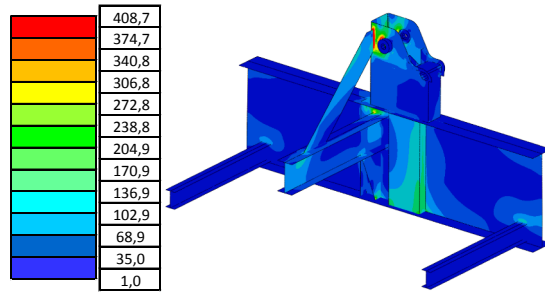


Fig. 44. Von Mises stresses (MPa), when applying 3-T loads to the new axle bracing assembly, including two type B supports.

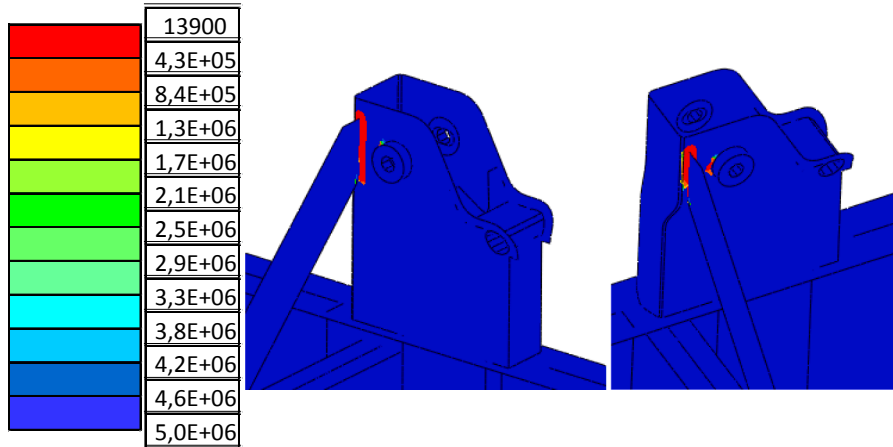


Fig. 45. Fatigue life prediction for 3-T load case and 50% survival probability for straight-shaped support in the new axle bracing assembly.

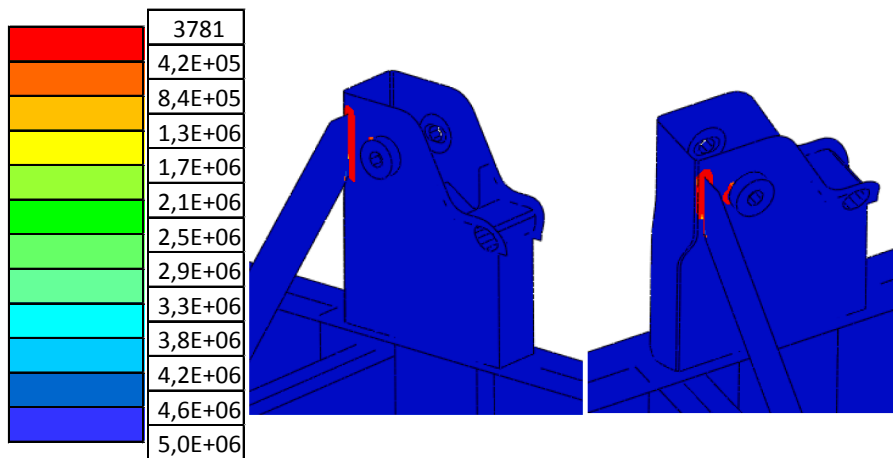


Fig. 46. Fatigue life prediction for 3-T load case and 95% survival probability for straight-shaped support in the new axle bracing assembly.

Declaration of Competing Interest

The authors declare that there is no conflict of interest.

Acknowledgments

This work was funded by the Spanish Ministry of Economy and Competitiveness under project no. TRA2012-2015-38826 (“Optimum Design of Lightened Buses and Semi-trailers based on Fatigue Life Prediction by Means of Virtual Testing procedures and Real-Time Data”). The authors would like to thank LECITRAILER S.A. for providing the axle bracing assembly.

Table 12
Fatigue life results.

	Numerical fatigue life prediction: 50% survival probability. (cycles)	Numerical fatigue life prediction: 95% survival probability. (cycles)	Experimental fatigue life. (cycles)
First axle bracing assembly, including straight and curved-shaped supports. Sinusoidal load applied: $-3.5/3.5T$.	10,300	2,802	640
Second axle bracing assembly, including only straight-shaped supports. Sinusoidal load applied $-3/3T$.	13,900	3,781	14,643

Table 13
Von Mises stresses for 3.5-T load fatigue test.

Load (Tons)	SS1-Mean stress S1 (MPa)	SS2-Mean stress S2 (MPa)	Von Mises equivalent stress (MPa)
3.5	100	20	91.7
-3.5	-15	-90	83.5

Appendix A. Supplementary material

Supplementary data to this article can be found online at <https://doi.org/10.1016/j.engfailanal.2019.104268>.

References

- [1] Srinivas Kodyialam, Multidisciplinary design optimisation - some formal methods, framework requirements, and application to vehicle design, *Int. J. of Vehicle Des.* 25 (1–2) (2001) 3–22, <https://doi.org/10.1504/IJVD.2001.001904>.
- [2] H.J. Beermann, *The Analysis of Commercial Vehicle Structures*, Mechanical Engineering Publications Limited, London, 1986.
- [3] UNE-EN ISO 6507-1:2018 “Metallic materials - Vickers hardness test - Part 1: Test method (ISO 6507-1:2018)”.
- [4] A. Wöhler, *Theorie rechteckiger eiserner Brückenbalken mit Gitterwänden und mit Blechwänden*, *Zeitschrift für Bauwesen* 5 (1855) 121–166.
- [5] O.H. Basquin, The exponential law of endurance test, *Proceedings of the American Society for Testing and Materials*, 1910, pp. 625–630.
- [6] Mischke, CR. *Journal of Mechanical Design-Transactions of the ASME*. Vol 104 Número: 3 Páginas: 653-660. DOI: 10.1115/1.3256401. IOWA State Univ SCI & Technol, Dept Mech Engr, AMES, IA 50011, USA. ASME-Amer Soc Mechanical ENG, 345 E 47TH ST, New York, NY 10017 ISSN: 0161-8458, 1982.
- [7] Society of Automotive Engineers, 1958, Nueva York, *Fatigue Design Handbook*, Vol. 4.
- [8] Besa A. J. y Giner E., 2003, “Componentes de Máquinas”, Pearsons Prentice Hall, Madrid.
- [9] J.E. Shigley, C.R. Mischke, R.G. Budynas, *Mechanical Engineering Design*, seventh ed., McGraw Hill Higher Education, 2003 ISBN 978-0-07-252036-1.
- [10] R.C. Juvinall, *Fundamentos de diseño para ingeniería mecánica*, Limusa, México, 1991.
- [11] J. Morrow, *Fatigue properties of metals*, section 3.2, *Fatigue Design Handbook*, Pub. No. AE-4. SAE, Warrendale, PA. 1999, 1968.
- [12] S.S. Manson, *Behavior of materials under conditions of thermal stress* (PDF), National Advisory Committee for Aeronautics NACA, 1953, p. TN-2933.
- [13] L.F. Coffin Jr., A study of the effects of cyclic thermal stresses on a ductile metal, *Trans. ASME*. 76 (1954) 931–950.
- [14] U. Muralidharan, S.S. Manson, A modified universal slopes equation for estimation of fatigue characteristics of metals, *ASME J. Eng. Mater. Technol.* 110 (1988) 55–58.
- [15] S.S. Manson, *Fatigue: a complex subject – some simple approximations*, *Exp. Mech. J. Soc. Experim. Stress Anal.* 5 (7) (1965) 193–226.
- [16] H. Malon, “Development of an innovative method for behavior analysis under fatigue loads of welded joints and structural components of semi-trailers”, *Doctoral Thesis*, University of Zaragoza. (Spain), 2010.
- [17] A. Hobbacher, *Recommendations for fatigue design of welded joints and components*, International Institute of Welding, 2008.
- [18] W.J. Kang, A.K. Kin, G.H. Kim, Fatigue failure prediction of press fitted parts subjected to a cyclic loading condition by finite element methods, *Fatigue Fract. Eng. Mater. Struct.* 30 (2007) 1194–1202, <https://doi.org/10.1111/j.1460-2695.2007.01188.x>.
- [19] Low cycle fatigue behaviour of welded T-joints in high strength steel. Schjødt-Thomsen J., Andreassen J.H. *Engineering Failure Analysis* 93 (2018) 38–43 <https://doi.org/10.1016/j.engfailanal.2018.06.026>. ISSN 1350-6307.
- [20] W. Weibull, A statistical distribution function of wide applicability“ (PDF), *J. Appl. Mech.-Trans. ASME* 18 (3) (1951) 293–297.
- [21] Papoulis, Pillai, “Probability, Random Variables, and Stochastic Processes”, 4th Edition.
- [22] W. Nelson, *Applied Life Data Analysis*, John Wiley & Sons, 1982.
- [23] <http://www.r-project.org/>.
- [24] K. Joreskog, Some contributions to maximum likelihood factor analysis, *Psychometrika* 32 (1967) 443–482.
- [25] T.W. Anderson, D.A. Darling, Asymptotic theory of certain goodness of fit criteria based on stochastic processes, *Ann. Math. Statist.* 23 (1952) 193–212.
- [26] K. Pearson, “On the criterion that a given system of deviations from the probable in the case of a correlated system of variables is such that it can be reasonably supposed to have arisen from random sampling, *Phil. Mag.* (5) 50, 157-175 Reprinted in K. Pearson 1956 (1900) 339–357.
- [27] A.N. Kolmogorov, Sulla determinazione empirica di una legge di distribuzione, *Giornale dell'Istituto Italiano degli Attuari* 4 (1933) 83–91.
- [28] M. Carrera, L. Castejón, E. Gil, C. Martín, C. Fabra, J.M. Olmos, Development of an innovative concept of light semi-trailer by means of FEM and testing, *SAE* (2004).
- [29] UNE-EN 10149-2. “Hot rolled flat products made of high yield strength steels for cold forming - Part 2: Technical delivery conditions for thermomechanically rolled steels”.
- [30] PNE-prEN 10027-2. “Designation systems for steels - Part 2: Numerical system”.
- [31] G. Spanos, D.W. Moon, R.W. Fonda, E.S. Menon, A.G. Fox, Microstructural, compositional, and microhardness variations across a gas-metal arc weldment made with an ultralow-carbon consumable, *Metal. Mater. Trans. A*. 32 (12) (2001) 3043–3054.
- [32] UNE-EN ISO 9015-1:2011. “Destructive tests on welds in metallic materials - Hardness testing - Part 1: Hardness test on arc welded joints (ISO 9015-1:2001)”.
- [33] UNE-EN ISO 18265:2014, “Metallic materials - Conversion of hardness values (ISO 18265:2013).
- [34] ISO 2394, “General principles on reliability for structures”, Second edition 1986-10-14.
- [35] EN 1993-1-9, “Design of steel structures-Part-1-9: Fatigue”, Eurocode 3, 2005.
- [36] W.N. Venables, B.D. Ripley, *Modern Applied Statistics with S, Statistics and Computing*, Springer, 2002.

- [37] N.M. Razali, Y.B. Wah, Power comparisons of shapiro-wilk, kolmogorov-smirnov, lilliefors and anderson-darling tests, *J. Statistical Model. Analyt.* 2 (1) (2011 Jan 1) 21–33.
- [38] J. Kalbeish, R.L. y Prentice, *The Statistical Analysis of Failure Life-time Data*, John Wiley & Sons, Inc., 2002.
- [39] J.F. Lawless, *Statistical Models and Methods for Lifetime Data*, John Wiley & Sons, Inc., 2003.
- [40] Gil Bellosta, C. J. (2011), “Anderson Darling GoF test with p value calculation based on Marsagliás 2004 paper (Evaluating the Anderson Darling Distribution)”, CRAN repository.
- [41] D. Valladares, M. Carrera, L. Castejon, C. Martin, Application of computational-experimental methods for designing optimized semitrailer axle supports, *Adv. Mech. Eng.*, 7 (1) (2015).
- [42] Failure analysis of fifth wheel coupling system. Y. Reboh, Sandro GrizaSandro Griza, A. RegulyA. Reguly, Telmo R. Strohaecker. *Engineering Failure Analysis* 15(2008):332-338. DOI: 10.1016/j.engfailanal.2007.02.007. ISSN 1350-6307.